

CROSS SECTION FOR THE PHOTOIONIZATION OF NOBLE-GAS ATOMS WITH ALLOWANCE FOR MULTIELECTRON CORRELATIONS

M. Ya. AMUS'YA, N. A. CHEREPKOV, and L. V. CHERNYSHEVA

Physico-technical Institute, USSR Academy of Sciences

Submitted August 7, 1970

Zh. Eksp. Teor. Fiz. 60, 160-174 (January, 1971)

The cross sections are obtained for the photoionization of the outer shell of Ne and two outer shells of the atoms Ar, Kr, and Xe with Hartree-Fock wave functions. Using these results as the zeroth approximation, we obtain the cross sections for photoionization with allowance for multi-electron correlations in the random-phase approximation with exchange. It is shown that these cross sections satisfy the sum rules and that the cross sections calculated with the aid of the matrix elements of the coordinate and of the momentum are equal. It is shown that the Hartree-Fock wave functions of the excited states, obtained in the field of the ion, take into account part of the diagrams of the random-phase approximation with exchange. The cross sections with allowance for multielectron correlations are in good agreement with experiment.

1. Interest in the allowance for multielectron correlations in the atom has increased recently^[1], owing to the large deviation of the results of the calculations in the single-particle Hartree-Fock approximation from experiment^[2]. To ascertain the role of multi-electron correlations in the atom, the authors have previously obtained the cross sections for the photoionization of the M and L shells of argon in the Hartree-Fock approximation^[3,4]. The discrepancy with experiment turned out to be large, particularly for the outer shell, and reached a factor of 2 and more. In the present paper we obtain the multiparticle corrections to the photoionization cross sections of the atoms Ne, Ar, Kr, and Xe, obtained in the Hartree-Fock approximation. To find the multiparticle corrections we used the high-density approximation, and concretely the random-phase approximation with exchange (RPAE)^[5]. It is shown that in this approximation there is satisfied a sum rule, according to which the integral of the photoionization cross section over the entire energy spectrum is proportional to the number of the electrons in the atom, and the cross sections $\sigma_{\text{RPAE}}^{\text{length form}}$ and $\sigma_{\text{RPAE}}^{\text{velocity form}}$ coincide^[6]. These relations do not hold in the Hartree-Fock approximation^[2,4].

The calculated cross sections for the photoionization of the outer shells of the atoms Ne, Ar, Kr, and Xe, with allowance for the multielectron correlations in the RPAE, differ from the experimental ones, as a rule, by not more than 10-15%.

2. In the single-particle approximation, when the wave function of the atom can be represented in the form of a Slater determinant made up of single-particle wave functions, the cross section for the photoionization of the n l-th subshell is determined by one of the formulas^[7] ($h = m = e = 1$):

$$\sigma_r^{nl}(\omega) = \frac{4\pi^2\alpha a_0^2}{3} \frac{N_{nl}\omega}{2l+1} [lR_{e,l-1}^2 + (l+1)R_{e,l+1}^2], \quad (1)$$

$$\sigma_v^{nl}(\omega) = \frac{4\pi^2\alpha a_0^2}{3\omega} \frac{N_{nl}}{2l+1} [lR_{e,l-1}^{(v)^2} + (l+1)R_{e,l+1}^{(v)^2}], \quad (2)$$

where

$$R_{e,l\pm 1} = \int_0^\infty P_{nl}(r) P_{e,l\pm 1}(r) r dr, \quad (3)$$

$$R_{e,l\pm 1}^{(v)} = \int_0^\infty P_{nl}(r) \left[\frac{d}{dr} P_{e,l\pm 1}(r) \pm \frac{2l+1\pm 1}{2r} P_{e,l\pm 1}(r) \right] dr, \quad (4)$$

N_{nl} is the number of electrons in the subshell, $\omega = \epsilon - E_{nl}$ is the energy of the photon in atomic units, $E_{nl} < 0$ is the energy of the electron prior to knock-out, $\alpha = 1/137$, and a_0 is the radius of the first Bohr orbit. The radial wave functions of the continuous spectrum are normalized to a δ -function of the energy and have the following asymptotic form:

$$P_{e,l}(r) \sim \sqrt{\frac{2}{\epsilon r}} \sin \left[\sqrt{2\epsilon} r - \frac{\pi l}{2} + \delta_l(\epsilon) \right] \quad (5)$$

In the case of a local single-particle potential, the velocity and momentum operators coincide:

$$\hat{v} = \hat{p}, \quad (6)$$

from which it follows^[7] that formulas (1) and (2) give identical results and that the following sum rule is satisfied:

$$S_0 \equiv \sum_{nl} \left[\sum_{n'l'} f_{nl \rightarrow n'l'} + \frac{1}{2\pi^2 \alpha a_0^2} \int_{I_{nl}}^\infty \sigma_{nl}(\omega) d\omega \right] = N, \quad (7)$$

where N is the number of electrons in the atom, I_{nl} is the ionization potential of the n l-th subshell, and $f_{nl \rightarrow n'l'}$ are the oscillator strengths for the transitions to discrete excited states. The experimental cross sections also satisfy the sum rule (7)^[8].

Equation (6) is not satisfied for a non-local single-particle potential. In the Hartree-Fock approximation, in which the exchange potential is non-local, we obtain in lieu of (6) the following relation for the matrix elements of the velocity and the momentum:

$$\begin{aligned} \langle k | \hat{v} | l \rangle &= i \langle k | \hat{H} \hat{r} - \hat{r} \hat{H} | l \rangle = i (E_k - E_l) \langle k | \mathbf{r} | l \rangle \\ &= \langle k | \hat{p} | l \rangle + i \sum_{n=1}^N \int \varphi_n^*(\mathbf{r}') \varphi_l(\mathbf{r}') \frac{(\mathbf{r} - \mathbf{r}')}{|\mathbf{r} - \mathbf{r}'|} \varphi_n(\mathbf{r}) \varphi_k^*(\mathbf{r}) d\mathbf{r} d\mathbf{r}'. \end{aligned} \quad (8)$$

Consequently formulas (1) and (2) are not equivalent in the Hartree-Fock approximation and the sum rule (7) is

not satisfied. For the cross sections $\sigma_{\mathbf{r}}$ we obtain in the Hartree-Fock approximation in lieu of (7)

$$S_0^{\mathbf{r}} = N + 2 \sum_{n, n_1}^N \int \varphi_{n_1}^*(\mathbf{r}') \varphi_n(\mathbf{r}') \frac{z(z-z')}{|\mathbf{r}-\mathbf{r}'|} \varphi_{n_1}(\mathbf{r}) \varphi_n^*(\mathbf{r}) d\mathbf{r} d\mathbf{r}' \delta_{s_n, s_{n_1}} \equiv N + \Delta S_0, \quad (9)$$

and for σ_{∇}

$$S_0^{\nabla} = N - \Delta S_0 + \sum_{n, n_1} \sum_{n'} \frac{2}{E_{n'} - E_n} \left| \int \varphi_{n_1}^*(\mathbf{r}') \varphi_n(\mathbf{r}') \times \frac{(z-z')}{|\mathbf{r}-\mathbf{r}'|} \varphi_{n_1}(\mathbf{r}) \varphi_n^*(\mathbf{r}) d\mathbf{r} d\mathbf{r}' \delta_{s_n, s_{n_1}} \right|^2, \quad (10)$$

where the summation over n' is carried out over all the excited states, and s_n is the projection of the spin in the state n . The last term in (10) is essentially positive and turns out to be smaller than ΔS_0 . Therefore, on the average $\sigma_{\mathbf{r}}$ can be larger than the experimental cross section, and σ_{∇} smaller. The difference between $\sigma_{\mathbf{r}}$ and σ_{∇} is a measure of the non-locality of the inter-electron interaction in the employed approximation.

Thus, the photoionization cross section in the Hartree-Fock approximation has two essential shortcomings: 1) the cross sections $\sigma_{\mathbf{r}}$ and σ_{∇} do not coincide, and the difference between them is large; 2) the sum rule (7) is not satisfied. In addition, as already indicated, it agrees poorly with experiment (see Figs. 6-9).

3. When considering the multielectron correlations in the atom, we shall use the formalism of many-body theory^[9]. A convenient zeroth approximation is the Hartree-Fock approximation, where it is necessary to choose for the unoccupied single-particle states the wave functions φ^{N+1} obtained in the field of the neutral atom, which are orthogonal to the functions of the occupied states and form together with the latter a complete system.

Estimates show that in medium and heavy atoms it is possible to use the high-density approximation^[10,11]. It is applicable in the case when the average distance between particles is much smaller than the effective radius of interaction between them. The condition for the applicability of the high-density approximation for the electron gas is the smallness of the parameter $\alpha = e^2/\pi p_0$ ^[5], where p_0 is the Fermi momentum, which is inversely proportional to the mean distance between the particles: $p_0 = (3\pi^2\rho)^{1/3}$, where ρ is the particle density. In the statistical approximation the radius of the atom is $R \sim Z^{-1/3}$, and therefore $p_0 \sim Z^{2/3}$. From this we obtain for large Z the estimate $\alpha \sim Z^{-2/3} \ll 1$.

The random-phase approximation (RPA) customarily employed in the case of high density, corresponds to a Hartree zeroth approximation. The method of random phases with exchange presupposes a Hartree-Fock zeroth approximation and is a generalization of the RPA method, making it possible to determine the perturbation-theory series at terms of higher order in the parameter α . Such a generalization, as applied to the atom, is very important, since the parameter α in the outer shells, which are of greatest interest from the point of view of the multi-electron correlations, while still smaller than unity, is not considerably smaller. The use of Hartree-Fock zeroth approximation makes it possible to take into account the inhomogeneity of the electron distribution in the atom already in the zeroth

approximation, but leads to the need for solving numerically the equations of the RPAE method¹⁾.

The cross section for photoionization with allowance for multi-electron correlations is determined in the RPAE approximation by the sum of infinite sequence of diagrams shown in Fig. 1, where a solid line corresponds to a particle or a hole, depending on the direction of the arrow, a wavy line corresponds to the Coulomb interaction, and a dashed line to the incident quantum. The square in this figure represents the interaction amplitude, which in the RPAE satisfies the equation

$$\langle k_1 k_3 | \Gamma(\omega) | k_2 k_4 \rangle = \langle k_1 k_3 | U | k_2 k_4 \rangle - \left(\sum_{\substack{k_5 \leq F \\ k_4 > F}} - \sum_{\substack{k_4 > F \\ k_5 \leq F}} \right) \frac{\langle k_1 k_6 | U | k_2 k_6 \rangle \langle k_3 k_3 | \Gamma(\omega) | k_6 k_4 \rangle}{\omega - E_{k_5} + E_{k_4} + i0(1 - 2n_{k_5})}, \quad (11)$$

where the index k_i denotes the set of four quantum numbers $n_l m_s$,

$$\langle k_1 k_3 | U | k_2 k_4 \rangle = \langle k_1 k_3 | V | k_2 k_4 \rangle - \langle k_1 k_3 | V | k_1 k_2 \rangle, \quad (12)$$

$\langle k_1 k_3 | V | k_2 k_4 \rangle$ are the Coulomb matrix elements:

$$\langle k_1 k_3 | V | k_2 k_4 \rangle = \int \varphi_{k_1}^*(\mathbf{r}_1) \varphi_{k_3}^*(\mathbf{r}_2) \varphi_{k_2}(\mathbf{r}_1) \varphi_{k_4}(\mathbf{r}_2) \frac{d\mathbf{r}_1 d\mathbf{r}_2}{|\mathbf{r}_1 - \mathbf{r}_2|}, \quad (13)$$

and n_{k_5} is the Fermi step function

$$n_{k_5} = \begin{cases} 1, & k_5 \leq F, \\ 0, & k_5 > F. \end{cases} \quad (14)$$

The condition $k_5 \leq F$ denotes summation over the occupied states, and $k_6 > F$ denotes summation over the free states, including integration over the continuous spectrum.

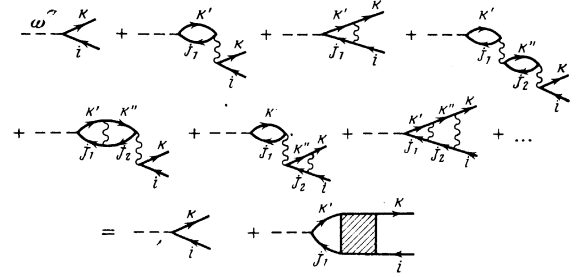


Рис. 1

After expansion of the Coulomb interaction in spherical functions and integration with respect to the angle variables, we obtain

$$\langle k_1 k_3 | V | k_2 k_4 \rangle = \sum_{l=0}^{\infty} \sum_{m=-l}^l (-1)^{m_1+m_3+m} \begin{pmatrix} l_1 & l & l_2 \\ -m_1 & -m & m_2 \end{pmatrix} \begin{pmatrix} l_3 & l & l_4 \\ -m_3 & m & m_4 \end{pmatrix} \cdot \langle n_1 l_1, n_3 l_3 || V_l || n_2 l_2, n_4 l_4 \rangle, \quad (15)$$

where the reduced matrix elements are defined as follows:

$$\langle n_1 l_1, n_3 l_3 || V_l || n_2 l_2, n_4 l_4 \rangle = \sqrt{(2l_1+1)(2l_2+1)(2l_3+1)(2l_4+1)} \begin{pmatrix} l_1 & l & l_2 \\ 0 & 0 & 0 \end{pmatrix} \times \begin{pmatrix} l_3 & l & l_4 \\ 0 & 0 & 0 \end{pmatrix} \left[\int_0^{\infty} dr_2 \int_0^{r_2} dr_1 P_{n_1 l_1}(r_1) P_{n_2 l_2}(r_1) \frac{r_1^l}{r_2^{l+1}} P_{n_3 l_3}(r_2) P_{n_4 l_4}(r_2) + \int_0^{\infty} dr_2 \int_{r_2}^{\infty} dr_1 P_{n_1 l_1}(r_1) P_{n_2 l_2}(r_1) \frac{r_1^l}{r_1^{l+1}} P_{n_3 l_3}(r_2) P_{n_4 l_4}(r_2) \right] \quad (16)$$

¹⁾ The results of [12,13], in which the cross section for the photoionization of the 4d¹⁰ subshell of Xe is considered, confirm the assumption that the high-density approximation is applicable to atoms with large Z .

Analogously, the matrix element of the interaction amplitude can be expanded in terms of the momentum transferred in the particle-hole channel:

$$\begin{aligned} & \langle k_1 k_3 | \Gamma(\omega) | k_2 k_4 \rangle \\ &= \sum_{l=0}^{\infty} \sum_{m=-l}^l (-1)^{m_1+m_3+m} \begin{pmatrix} l_1 & l & l_2 \\ -m_1 & -m & m_2 \end{pmatrix} \begin{pmatrix} l_3 & l & l_4 \\ -m_3 & m & m_4 \end{pmatrix} \\ & \quad \times \langle n_1 l_1, n_3 l_3 | \Gamma_1(\omega) | n_2 l_2, n_4 l_4 \rangle. \end{aligned} \quad (17)$$

We substitute expressions (15) and (17) in (11), multiplying by

$$(-1)^{m_1+m_3+m} \begin{pmatrix} l_1 & l & l_2 \\ -m_1 & -m & m_2 \end{pmatrix} \begin{pmatrix} l_3 & l & l_4 \\ -m_3 & m & m_4 \end{pmatrix}$$

and sum over m_1, m_2, m_3, m_4 . As a result we obtain an equation for the reduced matrix elements:

$$\begin{aligned} & \langle n_1 l_1, n_3 l_3 | \Gamma_1(\omega) | n_2 l_2, n_4 l_4 \rangle = \langle n_1 l_1, n_3 l_3 | U_1 | n_2 l_2, n_4 l_4 \rangle \\ & - \left(\sum_{\substack{n_3 \leq F, \\ n_4 > F}} - \sum_{\substack{n_3 > F, \\ n_4 \leq F}} \right) \frac{\langle n_1 l_1, n_3 l_3 | U_1 | n_2 l_2, n_4 l_4 \rangle \langle n_2 l_2, n_4 l_4 | \Gamma_1(\omega) | n_1 l_1, n_3 l_3 \rangle}{(2l+1)[\omega - E_{n_3} + E_{n_4} + i\delta(1-2n_n)]} \end{aligned} \quad (18)$$

where

$$\begin{aligned} & \langle n_1 l_1, n_3 l_3 | U_1 | n_2 l_2, n_4 l_4 \rangle = 2 \langle n_1 l_1, n_3 l_3 | V_1 | n_2 l_2, n_4 l_4 \rangle \\ & - \sum_{l'} (-1)^{l+l'} (2l+1) \begin{Bmatrix} l_1 & l & l_2 \\ l_3 & l' & l_4 \end{Bmatrix} \langle n_1 l_1, n_3 l_3 | V_{l'} | n_2 l_2, n_4 l_4 \rangle. \end{aligned} \quad (19)$$

The factor 2 in front of the first term on the right-hand side is the result of summation over spin projections which have been left out in the earlier calculations. In (18), summation was carried out over the spin projections in the initial state at six values in the final state.

In accordance with Fig. 1, the dipole matrix element, when account is taken of the multielectron correlations, is written as follows ($k_1 > F, k_2 \leq F$):

$$\langle k_1 | d | k_2 \rangle + \left(\sum_{\substack{k_2 \leq F, \\ k_1 > F}} - \sum_{\substack{k_2 > F, \\ k_1 \leq F}} \right) \frac{\langle k_4 | d | k_3 \rangle \langle k_4 k_2 | \Gamma(\omega) | k_3 k_1 \rangle}{\omega - E_{k_4} + E_{k_3} + i\delta(1-n_{k_4})}, \quad (20)$$

where $\omega = E_{k_1} - E_{k_2}$. The cross section for photoionization with allowance for multielectron correlations is determined by formulas (1) and (2), in which the matrix elements (3) and (4) should be replaced by the sum

$$\begin{aligned} & \langle n_1 l_1 | d | n_2 l_2 \rangle + \left(\sum_{\substack{n_3 \leq F, \\ n_4 > F}} - \sum_{\substack{n_3 > F, \\ n_4 \leq F}} \right) \frac{1}{3} \begin{pmatrix} l_3 & 1 & l_4 \\ 0 & 0 & 0 \end{pmatrix} \sqrt{\frac{(2l_3+1)(2l_4+1)}{(2l_1+1)(2l_2+1)}} \\ & \quad \times \frac{\langle n_4 l_4 | d | n_3 l_3 \rangle \langle n_4 l_4, n_2 l_2 | \Gamma_1(\omega) | n_3 l_3, n_1 l_1 \rangle}{\omega - E_{n_4} + E_{n_3} + i\delta(1-2n_n)}, \end{aligned} \quad (21)$$

in which $\langle n_1 l_1 | d | n_2 l_2 \rangle \equiv R_{\epsilon, l \pm 1}$ and is determined by one of the formulas (3) or (4).

4. We shall show that in the RPAE the photoionization cross section satisfies the sum rule (7), and the cross sections $\sigma_{\Gamma}^{\text{RPAE}}$ and $\sigma_{\nabla}^{\text{RPAE}}$ coincide. It is convenient to obtain the proof within the framework of the time-dependent Hartree-Fock approximation^[14], which is equivalent to the RPAE method^[15]. The wave function in this approximation has the form

$$|\Phi(t)\rangle = \exp(-iE_0 t) \exp\left(\sum_{i < F} \sum_{m > F} C_{mi}(t) a_m^+ a_i\right) |\Phi_0\rangle, \quad (22)$$

where Φ_0 is the ground state of the system in the Hartree-Fock approximation, E_0 is its energy, a_m^+ and

a_i are the operators of creation and annihilation of the particles, $C_{mi}(t)$ are complex coefficients, which can be represented in the form

$$C_{mi}(t) = X_{mi} e^{-i\omega t} + Y_{mi}^* e^{i\omega t}. \quad (23)$$

The coefficients X_{mi} and Y_{mi}^* do not depend on the time, and if $C_{mi}(t) \ll 1$ they satisfy the equations

$$(E_m - E_i) X_{mi} + \sum_{j < F} \sum_{n > F} (\langle mj | U | in \rangle X_{nj} + \langle mn | U | ij \rangle Y_{nj}) = \epsilon X_{mi}, \quad (24)$$

$$(E_m - E_i) Y_{mi} + \sum_{j < F} \sum_{n > F} (\langle ij | U | mn \rangle X_{nj} + \langle in | U | mj \rangle Y_{nj}) = -\epsilon Y_{mi},$$

where E_i is the energy of the single-particle state i in the Hartree-Fock approximation. We denote the solution of these equations, corresponding to the eigenvalue ϵ_n by the symbols X_{mi}^n and Y_{mi}^n , and the total wave function by $\Phi_n(t)$. The wave function of the ground state Φ_0 corresponds to a solution of (24) with $\epsilon = 0$, and those of the excited states—with $\epsilon \neq 0$. Equations (24) are conveniently written in matrix form^[16]:

$$\begin{pmatrix} A & B \\ B^* & A^* \end{pmatrix} \begin{pmatrix} X^n \\ Y^n \end{pmatrix} = \epsilon_n \begin{pmatrix} X^n \\ -Y^n \end{pmatrix}, \quad (25)$$

where

$$\begin{aligned} A_{mi, nj} &= (E_m - E_i) \delta_{ij} \delta_{mn} + \langle mj | U | in \rangle, \\ B_{mi, nj} &= \langle mn | U | ij \rangle. \end{aligned} \quad (26)$$

The matrix elements of the single-particle operator between the time-independent RPAE wave functions are represented in the following form^[16]:

$$\langle \Phi_0 | \hat{M} | \Phi_k \rangle = \sum_{i < F} \sum_{m > F} [\langle i | \hat{M} | m \rangle X_{mi}^k + \langle m | \hat{M} | i \rangle Y_{mi}^k] \equiv (M \tilde{M}) \begin{pmatrix} X^k \\ Y^k \end{pmatrix}, \quad (27)$$

where $\langle i | \hat{M} | m \rangle$ are the matrix elements calculated between the Hartree-Fock single-particle wave functions (the symbol \sim denotes the transpose). It can be shown that the matrix elements of the single-particle operator satisfy the relation

$$2 \sum_k \epsilon_k |\langle \Phi_0 | \hat{M} | \Phi_k \rangle|^2 = \langle \Phi_0 | [\hat{M}, [\hat{H}, \hat{M}]] | \Phi_0 \rangle, \quad (28)$$

where \hat{H} is the exact Hamiltonian of the system, and the summation with respect to k is carried out over all the excited states^[16]. If we take for \hat{M} the dipole moment operator \hat{d}_Z of the atom, then the left-hand sides of (7) and (28) coincide. The double commutator in (28) can be easily calculated:

$$\begin{aligned} \langle \Phi_0 | [\hat{d}_z, [\hat{H}, \hat{d}_z]] | \Phi_0 \rangle &= \sum_{i,j} \langle \Phi_0 | [z_i, [\hat{H}, z_j]] | \Phi_0 \rangle \\ &= \sum_{i=1}^N \langle \Phi_0 | -i [z_i, \hat{p}_{z_i}] | \Phi_0 \rangle = N. \end{aligned} \quad (29)$$

Thus, the cross section σ_{Γ} satisfies the sum rule (7) in the RPAE.

To prove the equivalence of the cross sections σ_{Γ} and σ_{∇} , it is convenient to verify that the velocity and momentum operators coincide. Using the relations given above, we obtain (we use matrix notation)

$$\begin{aligned}
 & -i \langle \Phi_0 | \hat{v}_z | \Phi_k \rangle = \langle \Phi_0 | \hat{H}z - z\hat{H} | \Phi_k \rangle = -e_k \langle \Phi_0 | z | \Phi_k \rangle \quad (30) \\
 & = -e_k(z\tilde{z}) \begin{pmatrix} X^k \\ Y^k \end{pmatrix} = -e_k(z-\tilde{z}) \begin{pmatrix} X^k \\ -Y^k \end{pmatrix} = -(z-\tilde{z}) \begin{pmatrix} A & B \\ B^* & A^* \end{pmatrix} \begin{pmatrix} X^k \\ Y^k \end{pmatrix}
 \end{aligned}$$

o., changing over to the usual notation

$$\begin{aligned}
 & -i \langle \Phi_0 | v_z | \Phi_k \rangle = - \sum_{i < F} \sum_{m, n > F} \{ [(E_m - E_i) \delta_{ij} \delta_{mn} X_{mi}^k \\
 & + \langle jm | U | ni \rangle X_{nj}^k + \langle mn | U | ij \rangle Y_{nj}^k] \langle i | z | m \rangle \\
 & - [(E_m - E_i) \delta_{ij} \delta_{mn} Y_{mi}^k + \langle in | U | mj \rangle Y_{nj}^k + \langle ij | U | mn \rangle X_{nj}^k] \langle m | z | i \rangle \}. \quad (31)
 \end{aligned}$$

Using the density of the single-particle wave functions, we sum over one of the indices m and n . After summation, the expression simplifies to

$$\begin{aligned}
 \langle \Phi_0 | \hat{v}_z | \Phi_k \rangle & = -i \sum_{i < F} \sum_{m > F} \{ (E_m - E_i) [\langle i | z | m \rangle X_{mi}^k - \langle m | z | i \rangle Y_{mi}^k] \\
 & + \sum_{j < F} \int \frac{\varphi_i^*(\mathbf{r}_1) \varphi_j^*(\mathbf{r}_2) (z_2 - z_1) \varphi_m(\mathbf{r}_1) \varphi_i(\mathbf{r}_2) d\mathbf{r}_1 d\mathbf{r}_2}{|\mathbf{r}_1 - \mathbf{r}_2|} X_{mj}^k \\
 & + \sum_{j < F} \int \frac{\varphi_i^*(\mathbf{r}_1) \varphi_m^*(\mathbf{r}_2) (z_2 - z_1) \varphi_j(\mathbf{r}_1) \varphi_i(\mathbf{r}_2) d\mathbf{r}_1 d\mathbf{r}_2}{|\mathbf{r}_1 - \mathbf{r}_2|} Y_{mj}^k \}. \quad (32)
 \end{aligned}$$

The matrix elements of the coordinate and of the momentum are connected in the Hartree-Fock approximation by relation (8). Substituting it in (32), we get

$$\langle \Phi_0 | \hat{v}_z | \Phi_k \rangle = \sum_{i < F} \sum_{m > F} [\langle i | \hat{p}_z | m \rangle X_{mi}^k + \langle m | \hat{p}_z | i \rangle Y_{mi}^k] = \langle \Phi_0 | \hat{p}_z | \Phi_k \rangle. \quad (33)$$

It follows therefore that in the RPAE approximation the cross sections σ_F and σ_V are equal.

5. The numerical solution of Eq. (18) for the amplitude of the interaction, with the functions φ^{N+1} , encounters difficulties connected with the divergence of the diagonal matrix elements $\langle n_1 l_1, n_2 l_2 | V_0 | n_1 l_1, n_2 l_2 \rangle$ when $n_1 \leq F$ and $n_2 > F$, when the state n_2 is in the continuous spectrum. We shall show that the use of the functions $\varphi_{(i)\epsilon}^N(\mathbf{r})$ obtained in the field of the ion is equivalent to summation of RPAE-method diagrams^[3] diagonal in the hole state and directed forward in time, and in particular, summation of all those diagrams containing the indicated divergent matrix elements. The wave functions $\varphi_{(i)\epsilon}^N(\mathbf{r})$ satisfy the equation

$$\begin{aligned}
 & \left(-\frac{\nabla^2}{2} - \frac{Z}{r} + \sum_{j < F} \int \frac{|\varphi_j(\mathbf{r}')|^2 d\mathbf{r}'}{|\mathbf{r} - \mathbf{r}'|} \right) \varphi_{(i)\epsilon}^N(\mathbf{r}) \\
 & - \sum_{j < F} \int \frac{\varphi_j^*(\mathbf{r}') \varphi_{(i)\epsilon}^N(\mathbf{r}') d\mathbf{r}'}{|\mathbf{r} - \mathbf{r}'|} \varphi_j(\mathbf{r}) - \sum_{j < F} E_{j\epsilon}^i \varphi_j(\mathbf{r}) = \epsilon \varphi_{(i)\epsilon}^N(\mathbf{r}), \quad (34)
 \end{aligned}$$

where

$$E_{j\epsilon}^i = \langle ji | U | i\epsilon \rangle \quad (35)$$

are the nondiagonal parameters^[7]. The solution, expressed in terms of the Green's functions of the equation for φ_{ϵ}^{N+1} ,

$$\begin{aligned}
 & \left(-\frac{\nabla^2}{2} - \frac{Z}{r} + \sum_{j < F} \int \frac{|\varphi_j(\mathbf{r}')|^2 d\mathbf{r}'}{|\mathbf{r} - \mathbf{r}'|} \right) \varphi_{\epsilon}^{N+1}(\mathbf{r}) \\
 & - \sum_{j < F} \int \frac{\varphi_j^*(\mathbf{r}') \varphi_{\epsilon}^{N+1}(\mathbf{r}') d\mathbf{r}'}{|\mathbf{r} - \mathbf{r}'|} \varphi_j(\mathbf{r}) = \epsilon \varphi_{\epsilon}^{N+1}(\mathbf{r}), \quad (36)
 \end{aligned}$$

is of the form

$$\varphi_{(i)\epsilon}^N(\mathbf{r}) = \varphi_{\epsilon}^{N+1}(\mathbf{r}) - \sum_{j < F} \frac{\langle ji | U | i\epsilon \rangle \varphi_j(\mathbf{r})}{\epsilon - E_j - i\delta} + \sum_m \frac{\langle mi | U | i\epsilon \rangle \varphi_m^{N+1}(\mathbf{r})}{\epsilon - E_m + i\delta (1 - 2n_m)}. \quad (37)$$

The matrix elements of this integral equation contain the sought wave functions $\varphi_{(i)\epsilon}^N(\mathbf{r})$, a fact marked by the bar over the corresponding index. We substitute the solution of (37), obtained by iteration, into the dipole matrix element:

$$\begin{aligned}
 \langle \varphi_{(i)\epsilon}^N | d | \varphi_i \rangle & = \langle \varphi_{\epsilon}^{N+1} | d | \varphi_i \rangle + \sum_{m > F} \frac{\langle mi | U | i\epsilon \rangle}{\epsilon - E_m + i\delta} \langle \varphi_m^{N+1} | d | \varphi_i \rangle \\
 & + \sum_{m > F} \sum_{n > F} \frac{\langle ni | U | i\epsilon \rangle \langle mi | U | n \rangle}{(\epsilon - E_m + i\delta)(\epsilon - E_n + i\delta)} \langle \varphi_m^{N+1} | d | \varphi_i \rangle + \dots \quad (38)
 \end{aligned}$$

This expression corresponds to a definite sequence of the diagrams shown in Fig. 2, in which the state of the hole does not change. In addition, unlike in Fig. 1, the time sequence of the interactions in these diagrams is fixed, i.e., they are Goldstone diagrams^[17], whereas the diagrams of Fig. 1 are Feynman diagrams^[9]. These differences can be readily seen when expressions (38) and (20) are compared.

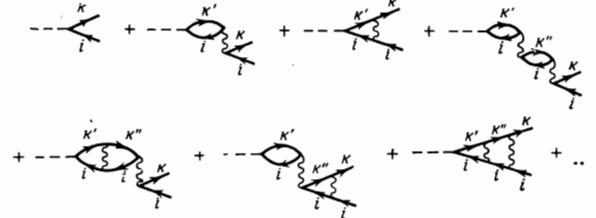


FIG. 2.

Equation (34) arises when the total wave function of the atom in the final state is sought in the form of one Slater determinant. Since in the final state there is one unfilled shell (besides the electron in the continuous spectrum), it follows that in order for the wave function to correspond to the state of the atom with definite values of the total angular momentum L and the spin S , it is necessary to seek it in the form of a linear combination of several Slater determinants, with different values of the angular momentum and spin projections of the particle and of the hole^[7]. We denote the wave function of the excited electron, corresponding to such a state of the atom, by the symbol $\varphi_{(i)\epsilon}^{N(LS)}(\mathbf{r})$. It can be shown that the use of the functions $\varphi_{(i)\epsilon}^{N(LS)}$ in place of φ_{ϵ}^{N+1} in the calculation of the photo-ionization cross section is equivalent to the summation of the Goldstone diagrams shown in Fig. 2, in which the hole belongs to one subshell, but can change the values of the angular momentum m and of the spin s .

In the numerical solution of the equations for $\varphi_{(i)\epsilon}^{N(LS)}$, the nondiagonal parameters were assumed equal to zero. Consequently, the functions $\varphi_{(i)\epsilon}^{N(LS)}$ turn out to be not orthogonal to the functions of the occupied states with the same l , and the second term on the right-hand side of (37) is missing, leading to the appearance of additional terms in the expansion (38). These terms correspond to diagrams not taken into account in the RPAE. However, as shown by a numerical analysis, the

contribution of these terms to the total cross section is small and does not exceed several per cent.

6. The use of the functions $\varphi_{(i)\epsilon}^N$ or $\varphi_{(i)\epsilon}^{N(LS)}$ in place of φ_{ϵ}^{N+1} in the calculation of the Coulomb matrix elements is also equivalent to summation of an infinite sequence of Goldstone diagrams of the RPAE method, analogous to those shown in Fig. 2. Therefore, when solving the equation for the interaction amplitude with such functions, it is necessary to discard the contribution of the terms already accounted for. We note that among the accounted-for terms are also those of the type shown in Fig. 3, where the double line corresponds to a particle described by the function $\varphi_{(i)\epsilon}^N$ or $\varphi_{(i)\epsilon}^{N(LS)}$. The contribution of the diagrams of Fig. 3 is contained in the term corresponding to the diagram of Fig. 4.

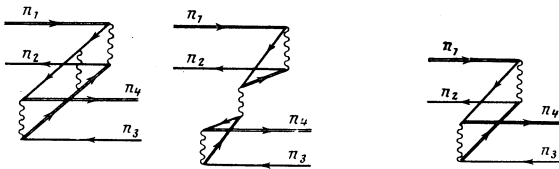


FIG. 3

FIG. 4

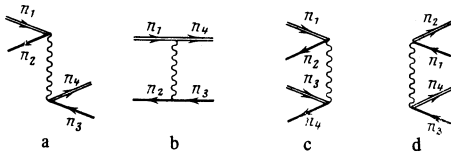


FIG. 5

In the equation for the interaction amplitude there are matrix elements of four types, shown in Fig. 5. The examples presented above show that when the functions $\varphi_{(i)\epsilon}^N$ are used as the zeroth approximation in (11), there is no need to take into account the contribution of the terms that contain matrix elements diagonal in the hole, shown in Figs. 5a and 5b. Subtraction of the contribution of such terms is equivalent to the solution of Eq. (11) with matrix elements $\langle k_1 k_3 | \bar{U} | k_2 k_4 \rangle$ in place of (12):

$$\langle k_1 k_3 | \bar{U} | k_2 k_4 \rangle = \langle k_1 k_3 | U | k_2 k_4 \rangle (1 - n_{k_1} \delta_{n_1 n_2} \delta_{l_1 l_2} \delta_{m_1 m_2} \delta_{s_1 s_2}) \times (1 - n_{k_2} \delta_{n_2 n_3} \delta_{l_2 l_3} \delta_{m_2 m_3} \delta_{s_2 s_3}). \quad (39)$$

If the wave functions $\varphi_{(i)\epsilon}^{N(LS)}$ are used as the zeroth approximation, then it is necessary to substitute in (11), in place of (12), the matrix elements $\langle k_1 k_3 | \bar{U}^{LS} | k_2 k_4 \rangle$:

$$\langle k_1 k_3 | \bar{U}^{LS} | k_2 k_4 \rangle = \langle k_1 k_3 | U | k_2 k_4 \rangle (1 - n_{k_1} \delta_{n_1 n_2} \delta_{l_1 l_2}) \times (1 - n_{k_2} \delta_{n_2 n_3} \delta_{l_2 l_3}). \quad (40)$$

In the numerical solution of the equation for the interaction amplitude, the integral with respect to the energy is replaced by a sum, which is terminated at a certain sufficiently large value of the energy. The integrand has a pole, and therefore the usual formulas of numerical integration were applied not to the sought integral, but to a difference, containing no pole, in the form

$$f(x) - r / (x - x_\lambda), \quad (41)$$

where r is the residue of the function $f(x)$ at the pole x_λ . As a result, the integral equation reduces to a sys-

tem of algebraic equations, the solution of which calls for inversion of the matrix^[18].

In the solution of the equation in the discrete spectrum, we took into account only the first excited state, and the contribution of the following levels was estimated and turned out to be small. The integral over the continuous spectrum was replaced by a sum of 11 terms. In this case, to solve Eq. (18) it is necessary to invert a matrix of order 48. The error in the determination of the matrix elements of the amplitude of the interaction turns out to be $\lesssim 10\%$. The calculations shown that, accurate to $\sim 10\%$, it is possible to neglect the interaction between the different states, for example, the interaction between the states $np^5 \epsilon d$ and $np^5 \epsilon s$ or $nd^9 \epsilon f$ and $nd^9 \epsilon p$, etc. Therefore Eq. (18) was solved for each subshell separately, and only the main transition, $np \rightarrow \epsilon d$ or $nd \rightarrow \epsilon f$, was taken into account. At the indicated accuracy, it suffices to determine the corrections to the photoionization cross section for the transitions $np \rightarrow \epsilon s$, $nd \rightarrow \epsilon p$, and $ns \rightarrow \epsilon p$ in the first order of perturbation theory, by substituting the Coulomb matrix element in expression (21) in place of the interaction amplitude.

7. The results of the calculations of the photoionization cross sections of the outer shells of the atoms Ne, Ar, Kr, and Xe are shown in Figs. 6–9, together with the experimental data. In the single-particle approximation, the results are given with the wave functions $\varphi_{(i)\epsilon}^{N(LS)}$. The cross sections $\sigma_R^{N(LS)}$ and $\sigma_V^{N(LS)}$ greatly differ from each other and from the experimental values, particularly in the vicinity of the ionization thresholds. At the same time it should be noted that the use of the single-particle wave functions φ^{HS} , obtained in the Herman-Skillman potential^[22], gives much worse results^[23,24], although the sum rule is satisfied for them and the cross sections σ_R^{HS} and σ_V^{HS} coincide. Thus, the cross section for the photoionization of the $4d^{10}$ subshell of Xe with the functions φ^{HS} has a very narrow maximum, equal to $140 \times 10^{-18} \text{ cm}^2$, whereas the experimentally observed broad maximum is equal to $30 \times 10^{-18} \text{ cm}^2$. The cross section σ^{HS} near the ionization threshold exceeds the experimental value (with the exception of Ne) by a factor of 2.

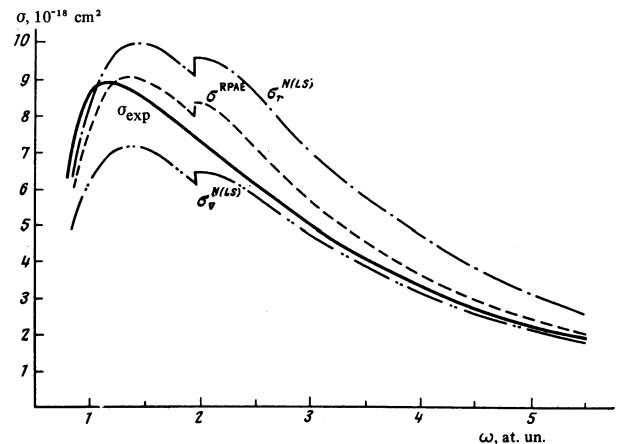


FIG. 6. Photoionization cross section of the L-shell of Ne. The experimental results are those of Samson^[8].

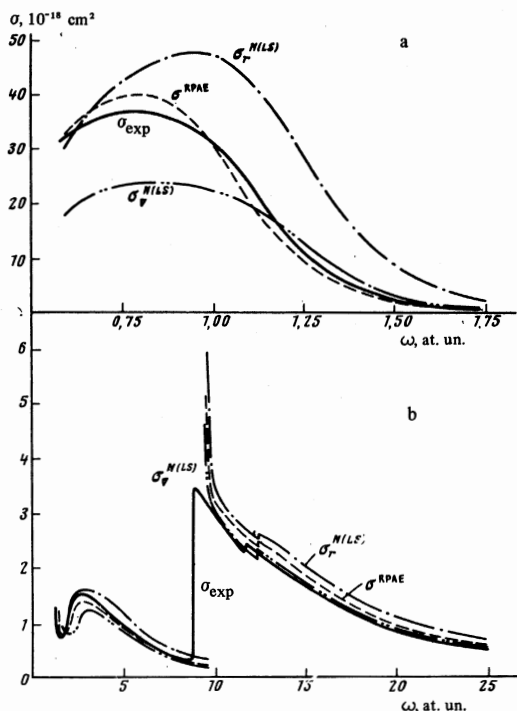


FIG. 7. Cross sections for the photoionization of the M shell (a) and L shell (b) of Ar. The experimental results are those of Samson [8] for the M shell and of Lukirskii and Zimkina [19] for the L shell.

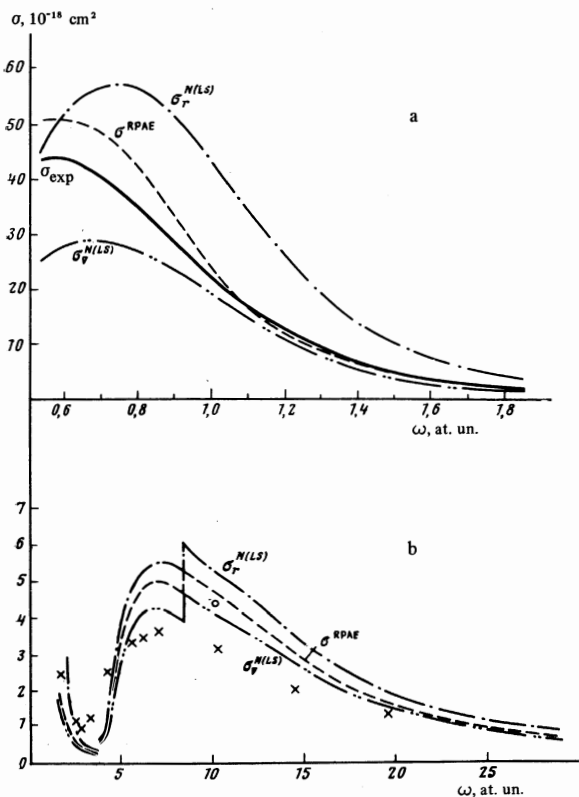


FIG. 8. Cross section for the photoionization of the N shell (a) and M shell (b) of Kr. Experimental data: solid line—Samson [8]; X—Lukirskii et al. [20]; O—Allen (taken from [8]).

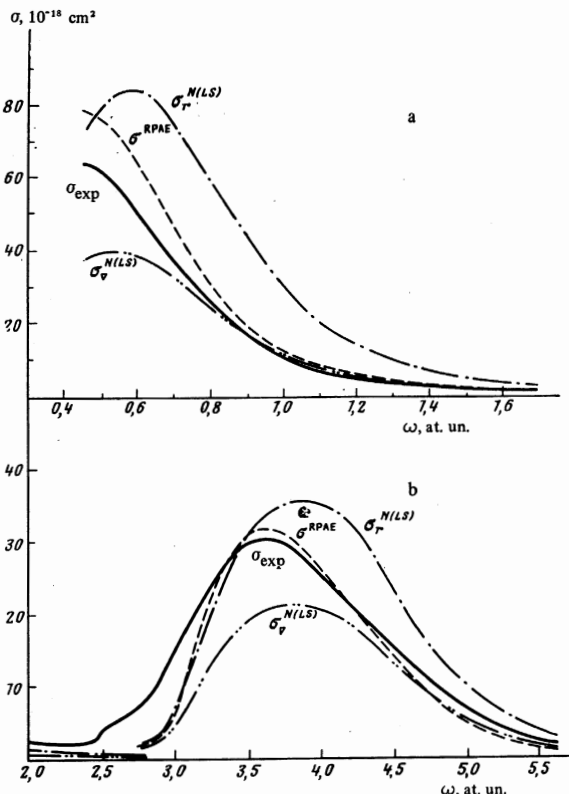


FIG. 9. Photoionization cross sections of the O shell (a) and the N shell (b) of Xe. The experimental data are those of Samson [8] for the O shell and of Ederer [2] for the N shell.

The photoionization cross sections with allowance for the multi-electron correlations in the RPAE approximation are in good agreement with experiment. Only at the ionization threshold of the L shell of Ar and for the $3d^{10}$ subshell of Kr do the deviations from experiment exceed 20%. The cross sections σ_{RPAE} and $\sigma_{\text{R}}^{\text{RPAE}}$ differ from each other on the average by 5%, and therefore we show in all the figures only one σ_{RPAE} curve. Satisfaction of this condition makes it possible to monitor the quality of the calculations. Proximity to the experimental curve ensures satisfaction of the sum rule for the σ_{RPAE} cross section.

Thus, the process of photoionization of the outer shells of the noble-gas atoms is entirely a many-particle process in the sense that it involves the participation of at least all the electrons of a given subshell. The use of the high-density approximation for the electrons of the outer shells give a satisfactory quantitative description of the photoionization process.

The results make it possible to impose more stringent requirements on the experimental data. The appearance of experimental data with accuracy $\sim 3-5\%$ would make it possible to obtain reliable information on the role of the corrections to the RPAE approximation

Note added in proof (30 November 1970). The authors thank Prof. Hansel for reporting new measurement results on the photoionization cross section of the M shell of krypton (P. Schreiber, DESY Preprint F41-70/5, June 1970). The cross section σ_{RPAE} shown in Fig. 8b differs from the reported one by not more than 15%.

used in this paper, and would by the same token yield very valuable information on the structure of multi-electron atoms.

The authors are deeply grateful to A. B. Migdal and L. A. Sliv for interest in the work, and also to S. I. Sheftel' and M. P. Kazachkov for numerous discussions and help.

¹Correlation effects in atoms and molecules, *Adv. Chem. Phys.* **14**, 1969.

²U. Fano and J. W. Cooper, *Rev. Mod. Phys.* **40**, 441, 1968.

³M. Ya. Amus'ya, N. A. Cherepkov, L. V. Chernysheva, and S. I. Sheftel', *Zh. Eksp. Teor. Fiz.* **56**, 1897 (1969) [*Sov. Phys.-JETP* **29**, 1018 (1969)].

⁴M. Ya. Amusia, N. A. Cherepkov, L. V. Chernysheva, and S. I. Sheftel, *Phys. Lett.* **28A**, 726, 1969.

⁵D. Pines and F. Nozieres, *Theory of Quantum Liquids*, Benjamin, 1966.

⁶M. Ya. Amusia, N. A. Cherepkov and L. V. Chernysheva, *Phys. Lett.* **31A**, 553, 1970.

⁷I. I. Sobel'man, *Vvedenie v teoriyu atomnykh spektrov (Introduction to the Theory of Atomic Spectra)*, Fizmatgiz, 1963.

⁸J. A. R. Samson, *Adv. Atomic Mol. Phys.*, **2**, 178, 1966.

⁹A. A. Abrikosov, L. P. Gor'kov, and I. E. Dzyaloshinskiĭ, *Metody kvantovoi teorii polya v statisticheskoi fizike (Quantum Field Theoretical Methods in Statistical Physics)*, Fizmatgiz, 1962 [Pergamon, 1965].

¹⁰W. Brandt and S. Lundqvist, *Phys. Rev.* **132**, 2135, 1963.

¹¹M. Ya. Amusia, *Phys. Lett.* **14**, 36, 1965.

¹²W. Brandt, L. Eder and S. Lundqvist, *J. Quant. Spectrosc. Radiat. Transfer*, **7**, 185, 411, 1967.

¹³M. Ya. Amusia, N. A. Cherepkov and S. I. Sheftel, *Phys. Lett.* **24A**, 541, 1967.

¹⁴D. J. Thouless, *Quantum Mechanics of Many-body Systems*, Academic, 1961.

¹⁵J. Goldstone and K. Gottfried, *Nuovo Cim.* **13**, 849, 1959.

¹⁶D. J. Thouless, *Nucl. Phys.* **22**, 78, 1961.

¹⁷J. Goldstone, *Proc. Roy. Soc.* **A239**, 267, 1957.

¹⁸C. Bloch, *Proc. Scuola Internazionale di Fisica "E. Fermi"*. Course XXXVI, New York, London, 1966, p. 393.

¹⁹A. P. Lukirskiĭ and T. M. Zimkina, *Izv. AN SSSR Seriya fiz.* **27**, 817 (1963).

²⁰A. P. Lukirskiĭ, I. A. Brytov and T. M. Zimkina, *Opt. Spektrosk.* **17**, 438 (1964).

²¹D. L. Ederer, *Phys. Rev. Lett.* **13**, 760, 1964.

²²G. Herman and S. Skillman, *Atomic Structure Calculations*, Prentice-Hall Inc., Englewood Cliffs, 1963.

²³E. M. McGuire, *Phys. Rev.* **175**, 20, 1968.

²⁴S. T. Manson and J. W. Cooper, *Phys. Rev.* **165**, 126, 1968.

Translated by J. G. Adashko